Volume 15, Issue 4, 152432 (1-9)

International Journal of Nano Dimension (IJND)

https://dx.doi.org/10.57647/j.ijnd.2024.1504.32

Microfluidic approach for the synthesis of silver nanoparticles (AgNPs) as promising antimicrobial agent

Raffaele Conte[1,2,*], Anna Valentino[1,2], Silvia Romano[1,3], Sorur Yazdanpanah[1,4], Fatima Ez-Zahra Amrati[5], Fahd Kandsi[6], Anna Calarco[1,2,7]

[1]*National Research Council-Research Institute on Terrestrial Ecosystems. Via Pietro Castellino, Naples, Italy.*
[2]*National Biodiversity Future Center (NBFC), Palermo, Italy.*
[3]*Elleva Pharma S.R.L. Via Pietro Castellino, Naples, Italy.*
[4]*Department of Experimental Medicine, Biotechnology and Molecular Biology Section, University of Campania " Luigi Vanvitelli", Naples, Italy.*
[5]*Laboratory of Cell Biology and Molecular Genetics (LBCGM), Department of Biology, Faculty of Sciences, Ibn Zohr University, Agadir, Morocco.*
[6]*Université Mohammed Premier, BV Mohammed VI B.P. Oujda, Morocco.*
[7]*UniCamillus-Saint Camillus International University of Health Sciences, Rome, Italy.*

[*]**Corresponding author:** raffaele-conte@cnr.it

Original Research

Received:
30 May 2024
Revised:
14 July 2024
Accepted:
19 July 2024
Published online:
10 October 2024

Abstract:

Silver nanoparticles (AgNPs) have emerged as promising agents in biomedical research due to their unique physicochemical properties and versatile applications. This study focuses on the synthesis of AgNPs using a microfluidic platform, optimizing reaction parameters to achieve monodisperse nanoparticles with a hydrodynamic diameter of approximately 129 nm and a stable negative zeta potential. Characterization techniques including dynamic light scattering and nanoparticles tracking analysis confirmed the size distribution and stability of the synthesized AgNPs. Evaluations of antibacterial activity demonstrated effective inhibition of *Staphylococcus aureus*, *Escherichia coli*, and *Pseudomonas aeruginosa* over 72 hours. Biocompatibility assessments on human keratinocytes revealed no cytotoxic effects, supporting the potential of AgNPs for safe biomedical applications. This comprehensive study underscores the significance of AgNPs in nanomedicine, highlighting their role in combating bacterial infections and their promising prospects in therapeutic applications.

Keywords: Antibacterial activity; Biocompatibility; Microfluidic synthesis; Nanomedicine; Silver nanoparticles

1. Introduction

In recent years, the rapid and widespread advancements in nanosciences and nanotechnology have significantly expanded the applications of nanomaterials across various fields. Nanomaterials, with their promising physicochemical properties, have enhanced the efficiency and performance of a wide array of materials and applications, fostering immense technological and economic prospects. Significant technological progress has been made in areas such as environmental remediation, electronics, cosmetics, structural materials, and biomedical sciences, medical diagnostics, imaging, and cancer therapy [1]. Among these, silver nanoparticles (AgNPs) have garnered significant attention in the biomedical field due to their advantageous properties, such as small size, elevated surface area to volume ratio, and biocompatibility [2]. Their pronounced efficacy against a broad spectrum of bacteria and viruses makes them invaluable in various medical applications.For example, Shahnaz Majeed et al. produced silver nanoparticles conjugating trans-activator of transcription (TAT) peptide with potential cytotoxic activity against MDA-MB-231 breast cancer cells

[3]. Research indicates that smaller silver nanoparticles exhibit stronger antibacterial effects compared to larger ones. This increased efficacy is attributed to the higher concentration of atoms on the surface, enhancing their reactivity and antimicrobial action [4, 5]. Consequently, silver nanoparticles are employed in numerous medical and healthcare applications. They are extensively utilized in drug delivery, diagnosis of diseases, wound healing, cosmetic treatments, and are commonly applied as coatings for medical devices, surgical tools, and implants [6].The synthesis of silver nanoparticles can be accomplished through various methods, with microfluidic technology being a particularly promising approach. Microfluidic systems, or lab-on-a-chip platforms, manipulate small fluid volumes and are typically made from transparent, chemically compatible, and biocompatible plastic materials [7]. These systems offer precise control over reaction conditions, ensuring reproducibility and the desired size and morphology of nanoparticles (NPs). Microfluidic is cost-effective and scalable, making it ideal for producing silver nanoparticles with specific characteristics needed for advanced biomedical applications [8]. This study explores the use of a t-shaped microfluidic system for the efficient on chip synthesis of these NPs. The synthetic process involves reducing silver ions in the presence of sodium hydroxyde (NaOH) and glucose at 25 °C, followed by comprehensive characterization to determine particle size, zeta potential, and hydrodynamic radius. Aim of this investigation is to optimize the synthesis process and enhance the desirable properties of silver nanoparticles for antibacterial-based advanced biomedical applications.

2. Experimental section

2.1 Materials

Silver nitrate (99.9%, Sigma Aldrich), sodium hydroxide (both of p.a. purity, Sigma Aldrich) and D-glucose (p.a. purity, Sigma Aldrich) were purchased from Sigma-Aldrich and used without any further purification. Ultrapure water was produced by Milli-Q® Type 1 Ultrapure Water Systems (Merck Millipore). All of the buffers cells and chemicals were purchased from Sigma-Aldrich (St. Louis MO, USA), Thermo Fischer Scientific (Milan, Italy), Invitrogen (Waltham, MA, USA), Gibco (Grand Island, NY, USA).

2.2 Microfluidic platform characteristic

Nanoparticles were synthesized using the automated Dolomite microfluidic platform (Dolomite, Royston, UK), provided of a T shaped Dolomite's glass Micromixer Chip with H interface connected by 0.25 mm FEP tubing to Mitos Duo XS-Pumps ($10-50$ μL/min and $100-500$ μL/min).

2.3 Synthesis

Silver nanoparticles were synthesized by directly reducing silver ions from a metallic precursor within a microfluidic platform. The microfluidic platform was designed in a cross shape with three inlet channels to optimize the reduction reaction. The silver precursor solution was introduced through the central inlet, while the other two inlets were designated for the organic reduction solution. The experiment was conducted using different concentrations of $AgNO_3$ in the final reaction mixture. The flow rates of the individual peristaltic pump channels were adjusted to different settings, as detailed in result and discussion paragraph. In the optmized conditions a 0.03 M $AgNO_3$ aqueous solution reacts with a 0.25 M NaOH aqueous solution containing 1 g/L of D-glucose. The obtained AgNPs were collected through centrifugation at 14,000 rpm for 30 min (5718R, OHAUS, Nanikon, Switzerland).

2.4 Characterization

The hydrodynamic diameter of nanoparticles (with the derived size), along with the polydispersity index (PDI) and the surface charge (zeta potential) of AgNPs were measured on the collected nanoparticles using the methodology detailed in Conte et al. [9]. AgNPs were resuspended in ultrapure water and measured at the temperature of 25 °C with the Malvern Zetasizer (Malvern Instruments Ltd., Malvern, UK). The found dimensions were also confirmed by Nanoparticles Tracking Analysis "NTA" (NanoSight NS 300, Malvern Instruments, Amesbury, United Kingdom, UK). The reported values represent the average of three measurements taken from the same sample.

2.5 Dynamic light scattering (dls).

Dynamic light scattering is a technique that analyzes the velocity distribution of particle motion caused by Brownian motion through the measurement of the scattered light. "Zetasizer Ultra" by Malvern (Malvern Panalytical, Amesbury, UK) was used for the instrumental acquisiion while the hydrodynamic radius of the particle was calculated with the Stokes–Einstein equation. Sample was prepared diluiting ten microliters of AgNPs in 990 μL of ultrapure water.

2.6 Nanoparticles tracking analysis (nta).

Nanoparticle Tracking Analysis (NTA) is a sophisticated technique used to analyze and characterize nanoparticles suspended in liquid. It measures the hydrodynamic diameter of nanoparticles by analyzing their Brownian motion under a laser beam (448 nm) providing a quantitative count of the particles within the analyzed volume. For analysis, AgNPs were resuspended in ultrapure water to obtain a concentration ranging from $\sim$ 128–140 particles/mL. Instrumental acquisition was made with NTA (Malvern Panalytical Ltd., Malvern, Worcestershire, UK) elaborating five videos of about 60 seconds with NanoSight NTA software version 3.2. The temperature was fixed at 25 °C and ultrapure water was used as blank.

2.7 FTIR-ATR

FTIR-ATR spectra were recorded on a Perkin Elmer Spectrum 100 spectrophotometer, equipped with a Universal ATR diamond crystal sampling accessory. The spectra were acquired as an average of 64 scans in the range $4000-480$ cm^{-1}, with a resolution of 4 cm^{-1}. Prior to measurements, the samples were kept at 60 °C under vacuum for 24 h.

2.8 Antibacterial activity of agnps extract against pathogenic bacteria

The antimicrobial activity of the silver nanoparticles was assessed monitoring the bacterial growth rate of *Staphylococ-*

cus aureus (ATCC 25923; Gram-positive), *Escherichia coli* (ATCC 25922; Gram-negative) and *Pseudomonas aeruginosa* (ATCC 15442; Gram-negative). For the assay, a bacterial suspension of approximately 1×10^5 CFU/mL was inoculated in 200 μL liquid broth in a 96-well plate as demonstrated by Di Salle et al. [10]. Then, the plate was incubated at 37 °C and 200 rpm and, at scheduled times (24 h, 48 h, 72 h), the optical density (OD 600 nm) of bacterial suspensions was recorded in a microplate reader (Cytation 3). The experiments were performed in triplicates.

2.9 Biocompatibility

Human keratinocytes (HaCaT cell line) were cultured in Dulbecco's Modified Eagle Medium supplemented with 10% fetal bovine serum. The cells were maintained at 37 °C in a humidified incubator with 5% CO_2. For the experiment, cells were plated at a density of 0.6×10^5 cells/cm^2 and allowed to adhere overnight. Subsequently, the cells were maintained for 24 hours with 1 mg/mL of silver nanoparticles in cell culture media and UV sterilized (3 hours). Cells without treatment served as the negative control. Results from the treated samples were compared to the negative control to assess biocompatibility.

2.10 Mtt assay

Cellular viability was evaluated using the MTT assay, involving the compound 3-(4, 5-dimethylthiazol-2-yl)-2, 5-diphenyltetrazolium bromide (MTT). After removing the culture medium, the cells were treated with a 1 mg/mL MTT solution and incubated at 37 °C for 2 hours. Viable cells converted MTT into purple formazan crystals, which were then dissolved using 2-propanol. The absorbance of the resulting solution was measured at 595 nm with a Benchtop Multi-Mode Microplate Reader (Cytation 3, Biotek).

2.11 Statistical analysis

Statistical analysis was conducted using the software GraphPad Prism 7.0 (La Jolla, CA, USA). The data were expressed as the mean ± standard error of mean. Statistical variances were determined using one-way ANOVA followed by a Tukey's post-hoc correction for multiple comparisons.

3. Results and discussion

Metal-based nanomaterials have attracted considerable interest owing to their distinctive physicochemical and biological properties. Their remarkable antibacterial, antifungal, and antiviral potentials make them highly appealing for medical applications [11–13]. Among these, silver nanoparticles have emerged as pivotal agents in advanced biomedical applications, particularly in combating bacterial infections. Their potent antibacterial properties derive from their small size and elevated area to volume ratio, which enhance their reactivity against a wide range of pathogens, including antibiotic-resistant strains like MRSA [14]. AgNPs are utilized in various medical contexts such as wound care, where they effectively reduce bacterial colonization and promote faster wound healing by mitigating inflammation and supporting tissue regeneration. Additionally, AgNPs are integrated into coatings for medical devices, implants, and surgical tools to prevent biofilm formation and reduce the risk of device-related infections [15]. In dermatology, AgNPs are incorporated into topical formulations for treating skin infections, burns, and inflammatory conditions due to their broad-spectrum antimicrobial activity [16]. The synthesis of AgNPs using advanced techniques like microfluidic technology ensures precise control over their size, morphology, and stability, crucial for optimizing their antibacterial effectiveness.

3.1 Synthesis

Silver nanoparticles were synthesized in a controlled environment using a Dolomite microfluidic system, equipped with a T-shaped microfluidic chip. The device glass Micromixer Chip was connected by 0.25 mm FEP tubing to Mitos Duo XS-Pumps ($10-50$ μL/min and $100-500$ μL/min). Three inlets, each 0.4 meters in length, were employed to deliver the reactants: one supplied silver nitrate and the others two provided the mixture of D-glucose and sodium hydroxide. The manufacturing parameters—including middle flow speed, side flow speed, flow rate ratio (FRR), silver nitrate concentration (on a fixed concentration of the solution sodium hydroxide-Dglucose) were systematically improved to achieve monodispersity of nanoparticles. Initially, flow rate ratio was optimized using a fixed concentrations of silver nitrate (0.05 M) and of the mixture NaOH containing 1 g/L of D-glucose (0.25 M), as shown in Table 1

Subsequently, silver nitrate concentration and flow rates were further optimized (Table 2).

The ideal settings were identified as the reaction between 0.03 M $AgNO_3$ aqueous solution and a 0.25 M NaOH aqueous solution, containing 1 L g of D-glucose. The obtained nanoparticles were collected by cooling centrifugation (Frontiers 5718R, OHAUS, Milan, Italy) at 37000 rcf for 45 min at 4 °C, washed with deionized water, and stored at 4 °C until further assays.

The synthesis of AgNPs follows a three-step process: the re-

Table 1. Optimization of the flow rate ratio.

Middle stream (μL/min)	Side stream (μL/min)	Flow rate ratio	Nanoparticle size (nm)
10	100	0.1	159 ± 13
20	100	0.2	226 ± 11
30	100	0.3	325 ± 18
40	100	0.4	377 ± 19
50	100	0.5	451 ± 24
10	200	0.05	297 ± 17
20	200	0.1	161 ± 39
30	200	0.15	146 ± 22
40	200	0.2	237 ± 18
50	200	0.25	244 ± 19
10	350	0.028	324 ± 22
20	350	0.057	271 ± 16
30	350	0.086	182 ± 13
40	350	0.114	139 ± 12
50	**350**	**0.143**	**129 ± 11**

Table 2. Optmization of $AgNO_3$ concentration and of flow rates.

$AgNO_3$ concentration (M)	NaOH aqueous solution containing 1 g/L of D-glucose (M)	Middle stream (μL/min)	Side stream (μL/min)	Nanoparticle size (nm)	Polidispersivity (PDI)
0.01	0.25	25	175	146 ± 20	0.298
0.02	0.25	25	175	158 ± 19	0.307
0.03	0.25	25	175	143 ± 12	0.188
0.04	0.25	25	175	154 ± 22	0.209
0.05	0.25	25	175	163 ± 27	0.234
0.01	0.25	50	350	140 ± 15	0.121
0.02	0.25	50	350	135 ± 13	0.098
0.03	**0.25**	**50**	**350**	**129 ± 11**	**0.046**
0.04	0.25	50	350	131 ± 16	0.087
0.05	0.25	50	350	149 ± 21	0.103
0.01	0.25	30	210	139 ± 17	0.138
0.02	0.25	30	210	148 ± 19	0.116
0.03	0.25	30	210	132 ± 13	0.088
0.04	0.25	30	210	144 ± 21	0.109
0.05	0.25	30	210	143 ± 23	0.116
0.01	0.25	15	105	154 ± 19	0.456
0.02	0.25	15	105	132 ± 25	0.357
0.03	0.25	15	105	135 ± 20	0.241
0.04	0.25	15	105	139 ± 15	0.451
0.05	0.25	15	105	140 ± 27	0.484

duction of silver ions (Ag^+) to silver atoms (Ag°), their nucleation with the formation of initial nuclei and the growth into larger nanoparticles. In the presence of D-glucose (a weak reducing agent) and sodium hydroxide (which acts as both a reducing and stabilizing agent), the reactions proceed as described by equations in Figure 1 [17].

Here, "A" represents the silver precursor, and "B" represents the nuclei or growing particles. The autocatalytic nature of the growth process ensures that the newly formed nuclei contribute to further particle formation, leading to the generation of AgNPs. The precise control over the reaction parameters within the T-shaped microfluidic chip facilitates the efficient and reproducible synthesis of AgNPs [18].

3.2 Characterization

Dynamic light scattering (DLS) was employed to determine the hydrodynamic diameter distribution and zeta potential of silver nanoparticles in suspension. Data were confirmed by nanoparticles tracking analysis (NTA). DLS analysis revealed that AgNPs have the hydrodynamic diameter of approximately 129 nm (Figure 2 a). The zeta potential of the AgNPs was −46 mV (Figure 2 b). The optimized formulation exhibits narrow size distribution and a significantly high negative surface charge. This combination enhances stability by preventing aggregation, as the strong repulsive forces from the negative surface charge keep the particles apart [19]. Additionally, the size of the obtained nanoparticles is similar to the dimensions of other metal-based nano-devices [20, 21].

Such findings were confirmed by nanoparticles tracking analysis (Figure 3). In particular, the NTA measurement (Figure 3 a) shows a mean nanoparticle size of 83,8 ± 2,4 nm with the large population at 52,5 ± 1,7 nm (Figure. 3 b). The screenshot of the video (Figure 3 c) along with the intensity report of the NTA analysis (Figure 3 d) confirmed the narrow size distribution of the nanoparticles.

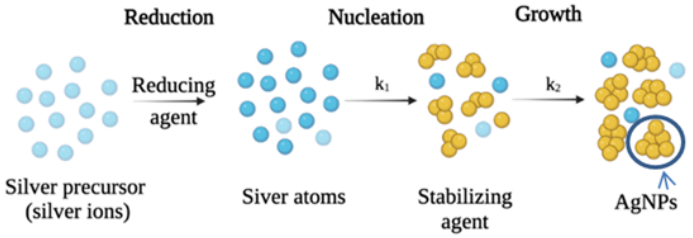

$$Nucleation: A \xrightarrow{k_1} B; \quad n_0 = k_1[A],$$

$$Growth: A + B \xrightarrow{k_2} 2B; \quad G = k_2[A][B],$$

Figure 1. Formation of silver nanoparticles.

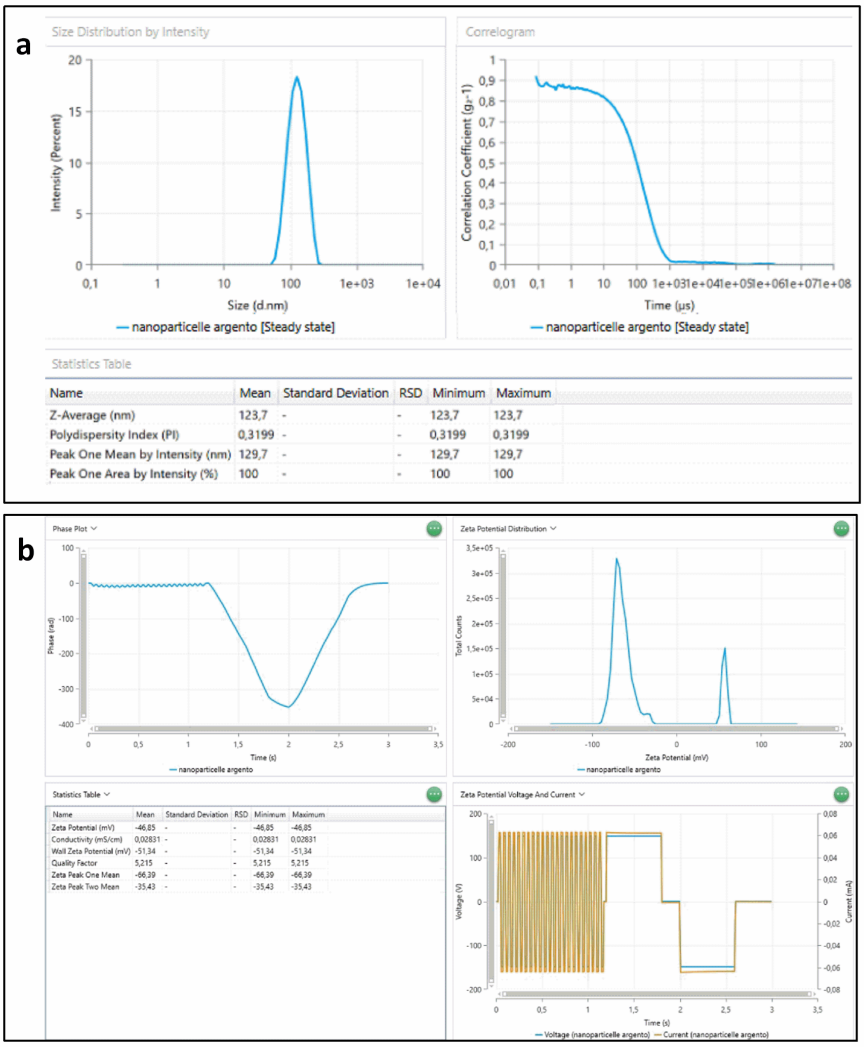

Figure 2. Size (a) and Z potential (b) of silver nanoparticles obtained through DLS measurement.

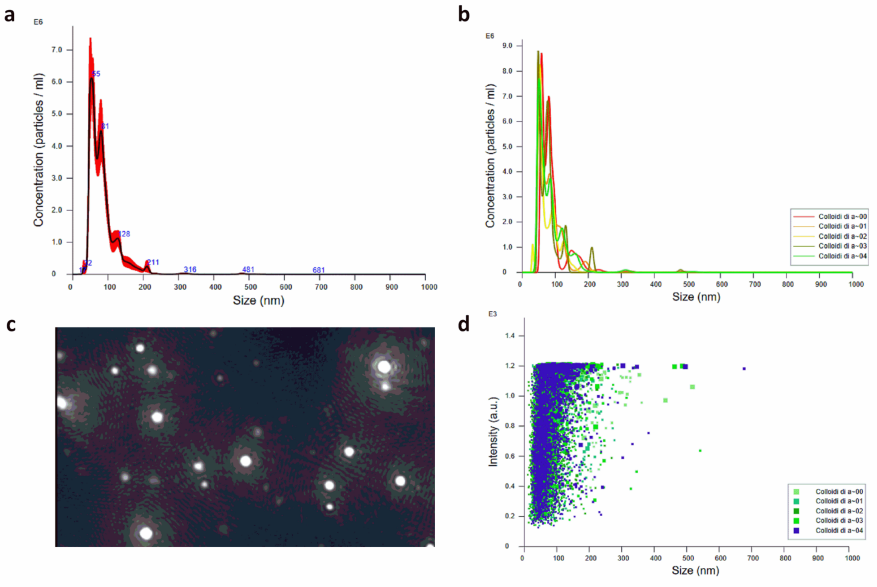

Figure 3. Representative images of: size (3a), population types (3b), screenshot of nanoparticles tracking analysis video (NTA, 3c), and distribution intensity (3d) of silver nanoparticles.

This observation not only validated the effectiveness of glucose in producing smaller silver nanoparticles but also underscored the importance of the choice of reducing agent in nanoparticle synthesis. The transformation of silver ions (Ag^{+}) to silver atoms (Ag°) was further confirmed using FTIR-ATR analysis (Figure 4). This is evidenced by a reduction in the intensity of the band at 1260 cm^{-1}, as well as a decrease in the sharp peak around 827 cm^{-1}, which correspond to the asymmetric and symmetric stretches of $-NO_3$ in silver nitrate, respectively.

Overall, the characterization provided valuable insights into the size, morphology, and structural properties of the synthesized silver nanoparticles. These findings are essential for understanding the underlying mechanisms governing nanoparticle synthesis.

3.3 Antibacterial activity of agnps against pathogenic bacteria

A significant challenge in treating infected sites is the bacterial colonization. Bacteria, once established, become more resistant to antibiotics and common biocides. To determine the effectiveness of AgNPs in addressing bacterial infection, it is essential to assess their impact on bacterial growth over different time intervals (24, 48, and 72 hours). For this purpose, *in vitro* experiments were conducted to evaluate the antibacterial properties of AgNPs. The evaluation focused on the growth dynamics of both Gram-positive and Gram-negative bacteria, namely *Staphylococcus aureus (S. aureus), Escherichia coli (E. coli)* and *Pseudomonas aeruginosa* (*PAO1*). These bacteria are well-known for their rapid proliferation and their potential to cause serious infections [22]. In particular, the antimicrobial activity of AgNPs was assessed in growth medium supplemented with 20% sucrose by monitoring the growth rate of *PAO1*, *S. aureus* and *E.coli* bacteria in the presence of the AgNPs (Bacterial growth without nanoparticles was used as control). The pH of the culture medium was monitored at various intervals, revealing that medium acidification begins as early as the first 9 hours of growth. This is attributed to the lactic acid produced by the bacteria, which causes a decrease in the environmental pH [23]. As shown in Figure 5 (a), AgNPs were able to inhibit the bacterial growth of *PAO1* (60%), *S. aureus* (59%) and *E.coli* (67%) after 1 hour. Inhibition plateaus at 48 hours and remains constant for up to 72 hours (Figure 5 b).

3.4 Biocompatibility

To assess the therapeutic potential of silver nanoparticles, it's crucial to establish their biocompatibility with human cells [24]. Specifically, this involves evaluating how these nanoparticles interact with human keratinocytes (HK). Keratinocytes are the primary cells of the skin, and testing on them helps determine if the nanoparticles can be used safely without causing harm, inflammation, or toxicity. Ensuring that silver nanoparticles are biocompatible with keratinocytes is essential for their safe application in medical treatments, particularly those involving direct contact with the skin. Figure 6 evaluates the impact of AgNPs on the viability of HK cells. According to the MTT assay results; there is no statistically significant difference in cell viability

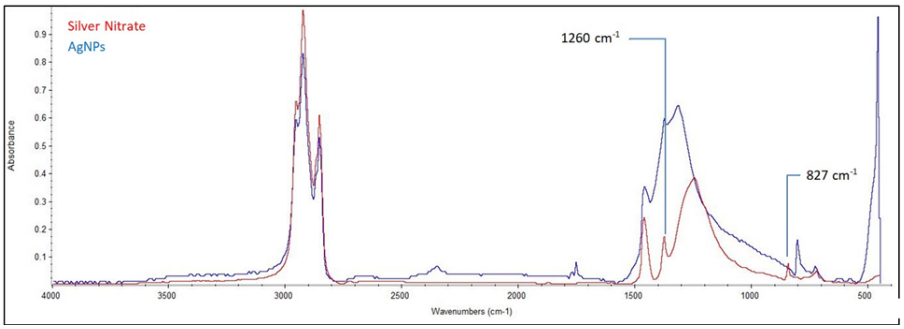

Figure 4. FTIR of silver nanoparticles.

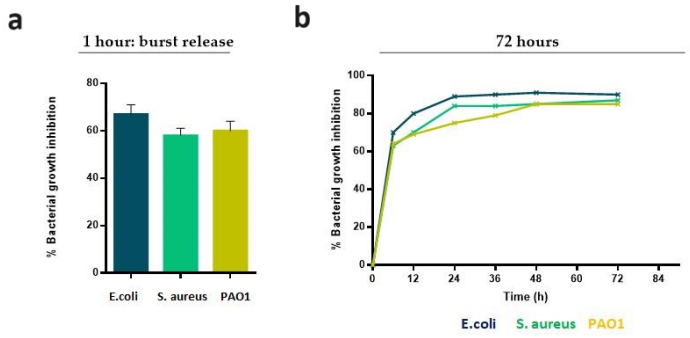

Figure 5. Antibacterial activity evaluated at 600 nm against *E.coli, S. aureus*, and *PAO1*. Bacterial growth without nanoparticles was used as controls. (a) 1 hours (b) until 72 hours. Each sample was measured in exaplicate and the results were reported as mean ± SD.

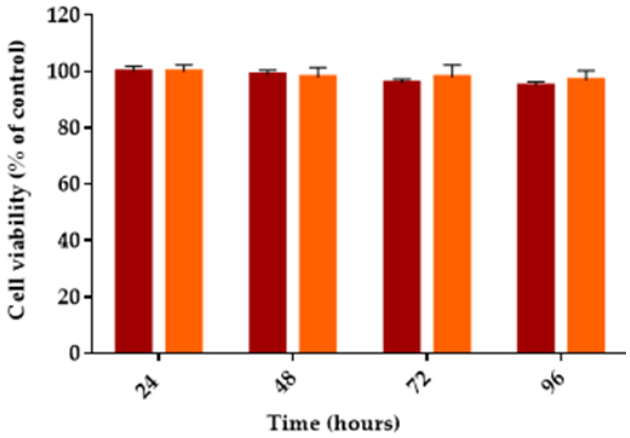

Figure 6. Effect of AgNPs on HK proliferation after 24, 48, 72 h, and 96 h for blank (red) and AgNPs (orange).

between cultures without nanoparticles (orange) and those cultured with silver nanoparticles (red).

4. Conclusion

In conclusion, this study highlights the synthesis and characterization of silver nanoparticles using a microfluidic platform. The synthesis process was meticulously optimized, involving the reduction of silver ions with D-glucose and sodium hydroxide. This method generated nanoparticles that are uniform in size, with a hydrodynamic diameter measuring approximately 129 nm. Furthermore, these nanoparticles exhibited a high negative zeta potential, indicating robust stability against aggregation.The antibacterial efficacy of these AgNps was demonstrated against pathogenic strains including *Staphylococcus aureus*, *Escherichia coli*, and *Pseudomonas aeruginosa*, showing significant inhibition of bacterial growth over 72 hours. The biocompatibility of the synthesized AgNPs was evaluated using human keratinocytes, revealing no adverse effects on cell viability. This finding is crucial as it suggests that the nanoparticles are safe for use in biomedical applications, highlighting their promising role in advanced medical therapies and biomedical devices.

Funding

This work was financially supported by: NextGenerationEU within the framework of National Biodiversity Future Center (NBFC); MUR-PRIN−2022 PNRR grant number P2022RZ8WM - Injectable Hydrogels for treatment of periodontal disease (HYPE). National Recovery and ResiliencePlan (NRRP), Mission 4 Component 2 Investment 1.4 - Call for tender No. 3138 of 16 December 2021, rectified by Decree n. 3175 of 18 December 2021 of Italian Ministry of University and Research funded by the European Union – NextGenerationEU; Award Number: Project code CN_00000033, Concession Decree No. 1034 of 17 June 2022 adopted by the Italian Ministry of University and Research.

Authors Contributions

Authors have contributed equally in preparing and writing the manuscript.

Availability of Data and Materials

The data that support the findings of this study are available from the corresponding author upon reasonable request.

Conflict of Interests

The authors declare that they have no known competing financial interests or personal relationships that could have appeared to influence the work reported in this paper.

References

[1] S. Hadi, S. S. Mohammad, J. Mehdi, A. Asaad, N. Masoud, Hamed, and A. Amirhossein. Genotoxicity assessment of carbon-based nanomaterials; have their unique physicochemical properties made

them double-edged swords. *Mutation Research/Reviews in Mutation Research*, 783(108296), 2020. DOI: https://doi.org/10.1016/j.mrrev.2020.108296.

[2] A. Naganthran, G. Verasoundarapandian, F. E. Khalid, M. J. Masarudin, A. Zulkharnain, N. M. Nawawi, M. Karim, C. A. Che Abdullah, and S. A. Ahmad. Synthesis, characterization and biomedical application of silver nanoparticles. *Materials*, 15(2):427, 2022. DOI: https://doi.org/10.3390/ma15020427.

[3] M. Shahnaz, S. Muthupandian, D. Mohammed, A. Z. Norul, N. M. I. Mohamad, H. R. Ezaz, N. A. Sharaf un, B. Hamed, K. M. Yugal, and M. Ebrahim. Bioengineering of green-synthesized tat peptide-functionalized silver nanoparticles for apoptotic cell-death mediated therapy of breast adenocarcinoma. *Talanta*, 253:124026, 2023. DOI: https://doi.org/10.1016/j.talanta.2022.124026.

[4] L. Xu, Y. Y. Wang, J. Huang, C. Y. Chen, Z. X. Wang, and H. Xie. Silver nanoparticles: synthesis, medical applications and biosafety. *Theranostics*, 10(20):8996–9031, 2020. DOI: https://doi.org/10.7150/thno.45413.

[5] F. Shahbazi, R. Ahmadi, M. Noghani, and G. Karimi. Antibacterial activity of the iron-zinc oxide nanoparticles synthesized via electric discharge method. *Inter. Journ. Nano. Dim.*, 14(1):60–72, 2023. DOI: https://doi.org/10.22034/ijnd.2022.1962974.2158.

[6] F. Paladini and M. Pollini. Antimicrobial silver nanoparticles for wound healing application: progress and future trends. *Materials (Basel).*, 12(16):2540, 2019. DOI: https://doi.org/10.3390/ma12162540.

[7] A. G. Niculescu, C. Chircov, A. C. Bîrcă, and A. M. Grumezescu. Fabrication and applications of microfluidic devices: a review. *Int J Mol Sci.*, 22(4):2011, 2021. DOI: https://doi.org/10.3390/ijms22042011.

[8] Bezelya, Ayşenur, Berrin Küçüktürkmen, and Asuman Bozkır. Microfluidic devices for precision nanoparticle production. *Micro*, 3(4):822–866, 2023. DOI: https://doi.org/10.3390/micro3040058.

[9] R. Conte, A. Valentino, F. Di Cristo, G. Peluso, P. Cerruti, A. Di Salle, and A. Calarco. Cationic polymer nanoparticles-mediated delivery of mir-124 impairs tumorigenicity of prostate cancer cells. *International Journal of Molecular Sciences*, 21, 2020. DOI: https://doi.org/10.3390/ijms21030869.

[10] A. Di Salle, G. Viscusi, F. Di Cristo, A. Valentino, G. Gorrasi, E. Lamberti, V. Vittoria, A. Calarco, and G. Peluso. Antimicrobial and antibiofilm activity of curcumin-loaded electrospun nanofibers for the prevention of the biofilm-associated infections. *Molecules*, 26:4866, 2021. DOI: https://doi.org/10.3390/molecules26164866.

[11] B. Hamed, J. Kamyar, P. Elaheh, M. Hamed, B. Negar, and V. Hossein. Chapter 17 - bioengineered metal-based antimicrobial nanomaterials for surface coatings,editor(s): aditya kumar, ajit behera, tuan anh nguyen, muhammad bilal, ram k. *Gupta, Antiviral and Antimicrobial Smart Coatings, Elsevier*, pages 489–539, 2023. DOI: https://doi.org/10.1016/B978-0-323-99291-6.00012-8.

[12] A. Vernet-Crua, D. Medina Cruz, E. Mostafavi, L. B. Truong, H. Barabadi, J. L. Cholula-Díaz, G. Guisbiers, and T. J. Webster. Chapter 11 - green-synthesized metallic nanoparticles for antimicrobial applications, editor(s): thomas j. webster. *Woodhead Publishing Series in Biomaterials, Nanomedicine (Second Edition)*, pages 297–338, 2023. DOI: https://doi.org/10.1016/B978-0-12-818627-5.00014-2.

[13] L. B. Truong, D. Medina-Cruz, J. J. Martínez-Sanmiguel, A. Soto-Mendoza, I. G. Esquivel-López, Y. Pérez, M. Saravanan, H. Barabadi, J. L. Cholula-Díaz, and E. Mostafavi. Chapter 8 - biogenic metal nanomaterials to combat antimicrobial resistance, editor(s): muthupandian saravanan, hamed barabadi, ebrahim mostafavi, thomas webster, in micro and nano technologies, emerging nanomaterials and nano-based drug delivery approaches to combat antimicrobial resistance. *Elsevier*, pages 261–304, 2022. DOI: https://doi.org/10.1016/B978-0-323-90792-7.00011-7.

[14] S. Dove Autumn, I. Dzurny Dominika, R. Dees Wren, Qin Nan, C. Nunez Rodriguez Carmen, A. Alt Lauren, L. Ellward Garrett, A. Best Jacob, G. Rudawski Nicholas, Fujii Kotaro, and M. Czyż Daniel. Silver nanoparticles enhance the efficacy of aminoglycosides against antibiotic-resistant bacteria. *Frontiers in Microbiology*, 13:1064095, 2023. DOI: https://doi.org/10.3389/fmicb.2022.1064095.

[15] Zimkhitha B. Nqakala, Nicole R. S. Sibuyi, Adewale O. Fadaka, Mervin Meyer, Martin O. Onani, and Abram M. Madiehe. Advances in nanotechnology towards development of silver nanoparticle-based wound-healing agents. *International Journal of Molecular Sciences*, 22(20):11272, 2021. DOI: https://doi.org/10.3390/ijms222011272.

[16] W. T. J. Ong and K. L. Nyam. Evaluation of silver nanoparticles in cosmeceutical and potential biosafety complications. *Saudi J Biol Sci.*, 29(4):2085–2094, 2022. DOI: https://doi.org/10.1016/j.sjbs.2022.01.035.

[17] M. Asif, R. Yasmin, R. Asif, A. Ambreen, M. Mustafa, and S. Umbreen. Green synthesis of silver nanoparticles (agnps), structural characterization, and their antibacterial potential. *Dose Response*, 20(2), 2022. DOI: https://doi.org/10.1177/15593258221088709.

[18] A. C. Bîrcă, O. Gherasim, A. G. Niculescu, A. M. Grumezescu, I. A. Neacșu, C. Chircov, B. Ș. Vasile, O. C. Oprea, E. Andronescu, M. S. Stan, C. Curuțiu, L. M. Dițu, and A. M. Holban. A microfluidic approach for synthesis of silver nanoparticles as a potential antimicrobial agent in alginate-hyaluronic acid-based wound dressings. *Int J Mol Sci.*, 24(14):11466, 2023. DOI: https://doi.org/10.3390/ijms241411466.

[19] R. Conte, I. De Luca, A. Valentino, P. Cerruti, P. Pedram, G. Cabrera-Barjas, A. Moeini, and A. Calarco. Hyaluronic acid hydrogel containing resveratrol-loaded chitosan nanoparticles as an adjuvant in atopic dermatitis treatment. *Journal of Functional Biomaterials*, 14(2):82, 2023. DOI: https://doi.org/10.3390/jfb14020082.

[20] M. Alimoradi, M. Yousefi, B. Sadeghi, M. M. Amini, and A. Abbasi. Structural and magnetic behavior of baal^{x}cr^{y}fe^{11}o^{19} (x+y=1) hexagonal ferrites. *J Supercond Nov Magn.*, 32:2533–2538, 2020. DOI: https://doi.org/10.1007/s10948-018-4980-5.

[21] J. Helmlinger, C. Sengstock, C. Groß-Heitfeld, C. Mayer, T. A. Schildhauer, M. Köllerb, and M. Epple. Silver nanoparticles with different size and shape: equal cytotoxicity, but different antibacterial effects. *RSC Adv.*, 6:18490–18501, 2016. DOI: https://doi.org/10.1039/C5RA27836H.

[22] Piatek, Magdalena, Cillian O'Beirne, Zoe Beato, Matthias Tacke, and Kevin Kavanagh. Pseudomonas aeruginosa and staphylococcus aureus display differential proteomic responses to the silver(i) compound, sbc3. *Antibiotics*, 12(2):348, 2023. DOI: https://doi.org/10.3390/antibiotics12020348.

[23] E. Yang, L. Fan, J. Yan, Y. Jiang, C. Doucette, S. Fillmore, and B. Walker. Influence of culture media, ph and temperature on growth and bacteriocin production of bacteriocinogenic lactic acid bacteria. *AMB Expr.*, 8:10, 2018. DOI: https://doi.org/10.1186/s13568-018-0536-0.

[24] M. Zielińska-Górska, E. Sawosz, M. Sosnowska, A. Hotowy, M. Grodzik, K. Górski, B. Strojny-Cieślak, M. Wierzbicki, and A. Chwalibog. Molecular biocompatibility of a silver nanoparticle complex with graphene oxide to human skin in a 3d epidermis in vitro model. *Pharmaceutics*, 14(7):1398, 2022. DOI: https://doi.org/10.3390/pharmaceutics14071398.